

Deposition of carbon nitride films by reactive sub-picosecond pulsed laser ablation

S. Acquaviva*, A. Perrone, A. Zocco
*Università di Lecce, Dip. di Fisica and Istituto Nazionale Fisica della Materia,
 Via per Arnesano CP 193, 73100 Lecce, Italy*

A. Klini and C. Fotakis
*Physics Department and Foundation for Research and Technology Hellas, Laser and Application Division
 P.O. Box 1527, 71110 Heraklion, Crete, Greece*

We have deposited, for the first time, CN_x films by sub-picosecond excimer laser ablation (KrF, $\lambda = 248$ nm, $\tau_L = 0.5$ ps) of graphite at 9 J/cm^2 laser fluence in different nitrogen pressures. In this paper we discuss the obtained film properties, as a result of several diagnostic techniques (scanning electron microscopy, profilometry, X-ray photoelectron spectroscopy, Fourier transform infrared and Raman spectroscopies), in terms of different physical mechanisms involved in reactive laser ablation process when graphite target is ablated in nitrogen atmosphere by lasers with different pulse duration. The deposition rate, the nitrogen concentration and the amount of the carbon, bounded to nitrogen atoms, are extremely reduced respects to the ones in the films deposited by nanosecond lasers. Moreover, the high particulate and droplet density, one of the worst drawbacks of laser deposition technique, is not decreased.

Keywords: Nitrides, Thin Films, Laser Ablation, Sub-picosecond Laser.

1. Introduction

Reactive pulsed laser ablation is well established as a universal tool for surface processing of materials and deposition of thin films of interest for modern technology.

Laser ablation process depends on physical properties of solid matter, laser parameters and environmental conditions. There are many parametric studies about the film properties in relation with the laser fluence [1], the wavelength [2] and the pulse duration. Since the physical mechanisms of laser-matter interaction change greatly with the laser pulse duration, one can distinguish different regimes (nanosecond/picosecond and femtosecond) [3-4].

The first step of the laser-matter interaction is the laser energy absorption that causes the heating of the bulk target. It depends not only on the intensity and the pulse duration, fixed laser fluence, but also on the kind of material, that is either absorbing (metal, semiconductor) or transparent (glass, plastic).

The energy absorption of a transparent target is characterised mainly by linear processes for nanosecond lasers and by non-linear processes for shorter pulses ($\tau_L < 200$ fs). In the last case [5] the creation of free charge carriers, by means of electron transitions between valence and conduction bands, is more probable to happen by multiphotonic absorption. In other terms, if a free electron acquires from laser photons higher energy than the band gap energy, it can ionise a lattice atom by collisions and bring another electron to the conduction band, creating free electrons in chain. There is ablation when free electron energy density is equal to binding energy of the lattice, corresponding to an electron concentration major than or equal to 10^{19} cm^{-3} . In the domain of femtosecond, the multiphotonic ionisation process is enough to have high electron density in conduction band and to induce ablation. Moreover, by using a shorter pulse laser, the time scale involved in the ablation with ps laser pulse is faster than

the energy transfer of electrons to crystalline lattice is (near to 1 ps).

For an absorbing target (i.e. the graphite in our case), the laser energy absorption is more probably linear, due to the high density of free electrons and valence electrons having an ionisation potential less than the photon energy [5]. However, it is crucial the role of pulse duration to determine the order of magnitude of the interaction region and the presence or not of a thermal affected zone, due to the heat diffusion. The laser energy is deposited in a surface layer whose thickness is of the order of the optical

penetration depth, $l_s = \frac{1}{\alpha}$, where α is the absorption

coefficient at a fixed wavelength. For long laser pulses (nanosecond regime), it is less than the thermal diffusion depth, $l_T = \sqrt{t_L \cdot D}$, where D is the diffusivity of the matter. So the material heats mainly for thermal diffusion and the ablation is accomplished by expulsion of fused material that solidifies again. As a consequence, one can see irregular structures in the morphology of the irradiated target surface [6]. As the laser pulse duration t_L decreases, the thermal diffusivity depth, l_T , decreases. When for a such t_L value as the thermal diffusion depth is less than the optical penetration depth, the second one determines the heated volume during the laser pulse. For ultra-short pulses (femtosecond regime), the energy deposited is limited in a layer with thickness of the order of the optical penetration depth and the localised energy heats the material faster from liquid to vapour phase than the irradiation by long pulses. As a consequence, at the pulse end the layer of the fused zone is very thin, because the most part of the heated material reaches rapidly the evaporation temperature (fast cooling), due to the steep temperature gradient.

So by shortening the laser pulse duration, from cw to fs, the thermal affected zone is smaller because of the

*: e-mail: acquaviva@le.infn.it

shorter interaction time, the energy loss into the sample is minimised and the ablation threshold is lower. Since little liquid is involved, ablation and material removal become highly precise, in contrast to the long pulse case [7]. However, what happens in the transition range, from ns to fs, is not clear and few papers are reported in literature. Up to now very few authors [8-9], have deposited films by sub-picosecond lasers. Few authors have reported about the ablation of material by lasers with pulse duration ≤ 200 fs [10] and the most of them have used the peculiarity of ultra-short lasers to have high precision patterning of the sample, without thermal damage of the surrounding, in the micromachining [11]. Moreover, there are no theoretical works about laser ablation deposition by short and ultra-short lasers.

In this paper we report the results obtained for the 0.5 ps excimer laser ablation of a graphite target in nitrogen atmosphere at different pressures. Our work was aimed by the interest in both the short laser ablation process and the deposition of carbon nitride films for their many applications (solar cell devices [12], optical or hard coatings [13]), due to the properties of high compressive strength, high optical transparency, high thermal conductivity and chemical inertness [14] of this compound. One expects that, reducing the melting phase, the irradiation by a short pulsed laser reduces the droplet formation and their presence on the deposited layer surface, which limits the quality [15-16] of the films grown by this technique. Really, at 0.5 ps, we are still in a thermal regime that is comparable to the nanosecond and in which the droplet formation is not avoided, as deduced by SEM analyses.

Furthermore, since our results show the drastic decrease of the deposition rate, going from tens ns to half ps, they are an experimental confirmation of the less ablation efficiency of the ps pulse respect to ns pulse, reported by Semerok et al. [17]. In the following sessions of the work we discuss the most significant experimental results about the morphological and chemical properties of the deposited films related to the different physical mechanisms involved in the ablation process, closely connected to the laser pulse duration.

2. Experimental results

Depositions were performed using a KrF excimer laser

($\lambda = 248$ nm, $\tau_L = 0.5$ ps). Series of 2×10^4 pulses at a repetition rate of 10 Hz were directed to high purity graphite targets which rotated with a frequency of 1 Hz to reduce fast drilling. The laser beam was incident on the target surface with an angle of 45° and the laser fluence was set at 9 J/cm^2 . The ablated material was collected on quartz or (100) silicon (p-type, resistivity of $0.001 - 0.008 \Omega \text{ cm}$) substrates at room temperature, placed in front of the target at a distance of 2.5 cm.

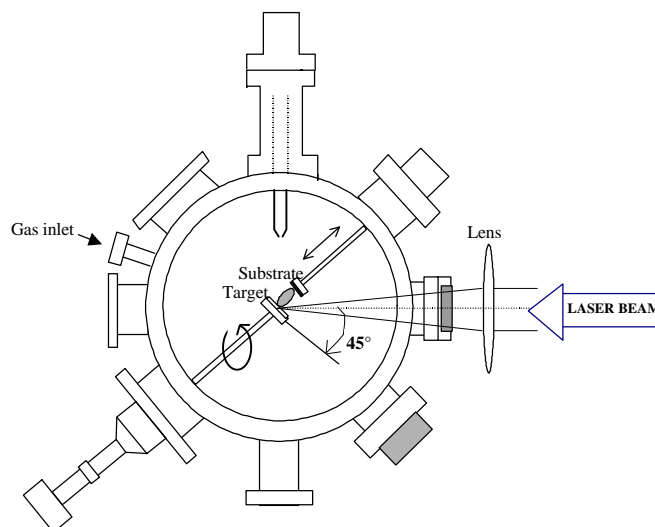


Fig. 1 Experimental apparatus

The stainless steel vacuum chamber was evacuated down 10^{-4} Pa and then filled with high purity nitrogen (electronic grade 99,999 %), continuously blown inside the chamber and set at a chosen pressure value in the 0.05-50 Pa range. A scheme of our experimental set-up is shown in fig. 1.

The deposited films show a good adhesion to both substrates. Their surface is free of cracks and corrugations. Droplets and particulates of submicron size are observed in whole range of N_2 pressure and they are sprayed over the film surface, as visible in the SEM micrographs reported in fig. 2. Their dimensions are in the range ($0.5-1 \mu\text{m}$) and do not change with the nitrogen pressure. Their high density seems to decrease as the nitrogen pressure increases. The SEM micrograph of film deposited at 0.05 Pa shows a morphological structure characterised by domains, probably due to the silicon dioxide that refines under the electron beam.

Density and particulate sizes are confrontable with the ones obtained for the films deposited by nanosecond laser [18]. So we can stress that in the sub-picosecond regime there is no clear improvement in the film morphology and that a melted phase could be still present.

The thickness of the deposited CN_x films is very low and not uniform. One can distinguish two separated regions characterised by different thickness values, as inferred from profilometry measurements (Tab. I).

Probably, this non-uniformity is due to the short substrate-target distance ($d=2.5$ cm) used to increase the low deposition rate in these experiments. The maximum deposition rate ($\sim 0.07 \text{ \AA/pulse}$) is one order of magnitude lower, on whole nitrogen pressure range, than the one obtained for films deposited by ns pulses and on substrates placed just at higher distance from the target. The very low deposition rate reveals worst ablation efficiency when one passes from 30 ns to 0.5 ps laser. In fact, previous CN_x

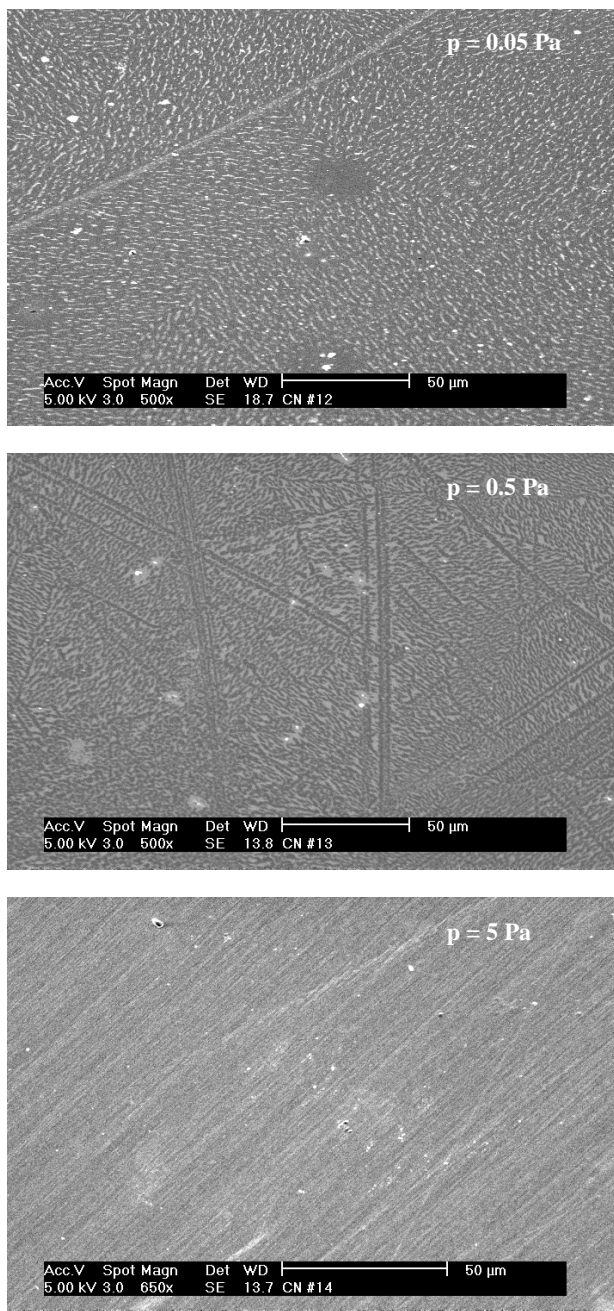


Fig. 2 SEM micrographs of the films deposited on silicon substrate at different nitrogen pressures.

Table. I Thickness of the films grown on silicon substrate at different nitrogen pressures.

	PN ₂ (Pa)	t (nm)	
		thin region	thick region
# 1	0.05	30	140
# 2	5	40	120
# 3	50	50	100

films, deposited at the same experimental conditions but by a ns laser, showed a deposition rate of 0.2 Å/pulse, even if the target-substrate distance was of 4 cm. At a shorter target-substrate distance, the thickness might become much higher, since the deposition rate is proportional to d^{-2} . In order to explain this different ablation efficiency for the two different pulse durations, one has to take in account the partial incoming laser energy absorption by the dense plasma. The entity of this absorption depends on both electronic and atomic density. In the case of 0.5 ps pulse, both densities are larger than the ones in the ns case and the plasma absorption is also bigger [19]. This fact reveals that the ps laser ablation of graphite is less efficient in deposition of CN_x thin films.

The RBS analyses confirm the very low thickness of the films. Moreover, the spectra indicate that the nitrogen concentration is very low in all deposited films (<15%). XPS spectra are mainly dominated by the C1s peak. There are also the N1s and O1s electron peaks, but they are characterised by a very low intensity indicating a low percentage concentration of nitrogen on the first 20 nm of the film surface layer. The films are nitrogen lacking: the N/C atomic ratio is of about 0.15 and doesn't change with the nitrogen pressure. In particular, the C1s electron deconvolution peaks (fig. 3) are at the binding energy of 285.0 eV, 286.3 eV and 288.2 eV attributed to C-O bond, sp covalent triple bond (C≡N) and sp³ covalent single bond (C-N), respectively. The N1s electron peak (fig. 3) is decomposed in two gaussian peaks at 399.0 eV and 400.2 eV, corresponding to the single N-C and to the double N=C bond, respectively. The FT-IR spectra, recorded by a Perkin Elmer Spectrum 2000 Fourier transform infrared spectrometer, in the 2000-4000 cm⁻¹ wavenumber range, do not change considerably with the nitrogen pressure. One

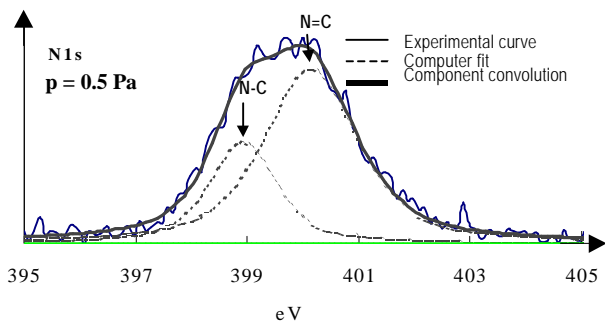
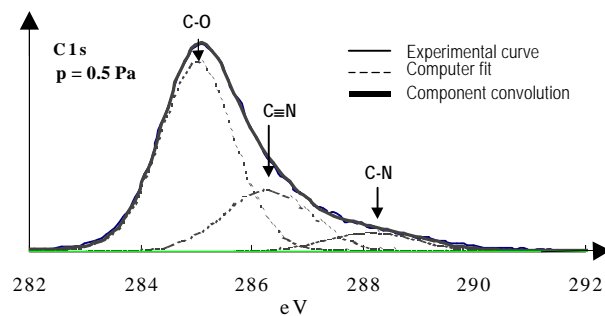


Fig. 3 X-ray photoelectron spectra of C1s and N1s electrons of the film deposited on silicon in 0.5 Pa-nitrogen.

can observe only a transmission band intensity increase, as the gas pressure increases from 0.05 to 5 Pa. In all our spectra the main feature is the band at 2200 cm^{-1} attributed to $\text{C}\equiv\text{N}$ triple bond stretching mode, but either the transmission band related to $\text{C}=\text{N}$ double bond stretching mode or the ones corresponding to $\text{C}-\text{N}$ single bond stretching mode or to $\text{C}=\text{C}$ double bond stretching mode cannot be seen, because the quartz of the substrate doesn't transmit in the region under 2000 cm^{-1} . However the sp^2 C atoms are assured by Raman spectroscopy.

In fact, in order to distinguish among different bond types, Raman spectroscopy was performed by directing an argon-ion laser (514.5 nm) beam with a power of some mW on the sample surface on a spot of $\approx 200\text{ }\mu\text{m}$, to minimise any possible beam heating effect and film graphitization. First order Stokes spectra were detected with a Spex double monochromator. From the acquired spectra it is possible to point out that the films contain mainly sp^2 sites. The main features of Raman spectra (fig. 4), obtained by fitting them with two Gaussian lineshapes and a linear background, are the D ("Disorder") and G ("Graphitic") bands, at about 1397 and 1570 cm^{-1} , respectively.

The first one is associated with the optically allowed E_{2g} zone centre mode of the crystalline graphite, the second one with a zone edge A_{1g} mode activated by disorder in the graphitic crystal [20]. Respect to the pure crystalline graphite Raman spectrum, consisting of two peaks centred on 1350 and 1550 cm^{-1} , the positions of these two features are shifted in higher wavenumber. It might be due to the removal of bond-angle disorder and the increasing dominance of crystallites. From Raman studies we can deduce that in the films there is a large amount of the graphite clusters (domains), a consequent large amount of the $\text{C}=\text{N}$ stretching vibrations and a disorder grade varying without a specific trend with the nitrogen pressure in the reaction chamber.

3. Discussion

The deposited films are very thin, graphitic and nitrogen lacking. The deposition rate is extremely reduced respect to the one obtained by nanosecond lasers [21-22]. It is due to the denser plasma absorption and the less ablated material as well [23]. Indeed, while the ablation efficiency, defined as ratio of ablated matter volume to the laser pulse energy, is better with shorter pulses (fs), the ns efficiency is better than the ps one. In fs regime, the pulse duration is shorter compared to a typical time ($\sim 1\text{ ps}$) of electron-phonon collision in solid matter, so the laser pulse finishes before the energy is redistributed in the solid. In this fs regime, the energy is deposited in the surface without laser-plasma interaction.

On the other hand, our regime of the 500 fs pulse duration is probably the same order or longer than the energy relaxation time, so the irradiated volume heating leads to vaporise the surface during the laser pulse and the plasma shielding can occur. By longer pulses, the ablated

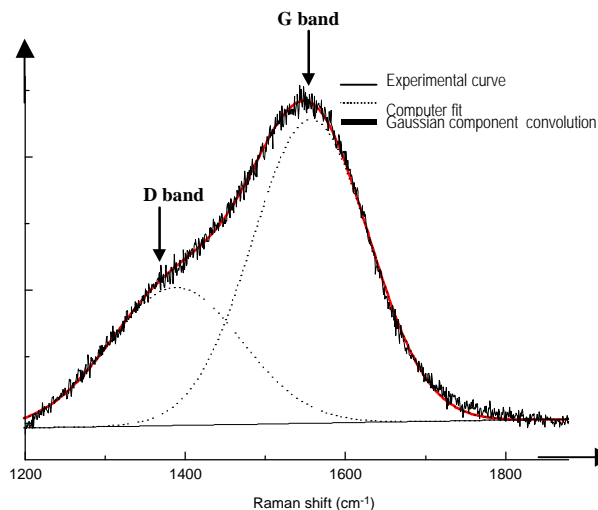


Fig. 4 Raman spectrum of the film deposited on silicon substrate in of 5 Pa-nitrogen atmosphere.

material increases, as a consequence of the ablated depth and the volume increasing. In fact, laser ablation should be considered a hydrodynamic process in which the vaporisation front moves into the solid during the pulse. Moreover, in this case (ns regime) one-photon ionisation absorption is dominant. On the contrary, with a ps pulse the laser intensity and the plasma particle density are larger so that the absorption (plasma shielding) is larger and, as a result, the ablation efficiency is lower.

The plasma shielding can also explain the reasons of very low nitrogen concentration in the deposited films. In fact, even if the multiphotonic ionisation is the most probable physical mechanism in the plasma plume produced by higher powered laser ablation, the velocity of the expelled chemical species can decrease due to the much higher plasma density, the lower free path of chemical species and the greater number of probable collisions.

Since it is accepted that the bonds between carbon and nitrogen, above all the sp^3 bond, are preferred when as energetic as possible species hit on the substrate surface, in our sub-picosecond regime the formation processes of CN_x compound could change respect to the ones obtained by ns pulse.

4. Conclusions

For the first time CN_x films have been deposited by sub-picosecond excimer laser ablation (KrF , $\lambda = 248\text{ nm}$, $\tau = 0.5\text{ ps}$) of graphite, at different nitrogen pressures.

The obtained films are thin, graphitic and very poor in nitrogen. The droplet and particulate density is as same as the one of the films deposited by nanosecond excimer laser ablation.

In short, the reactive pulsed laser ablation by 0.5 ps laser does not give the hoped improvements in the

morphology and composition of CN_x films. Therefore, the next step will be to study the properties of the CN_x films deposited by using fs lasers and to verify if the ablation efficiency and the film quality, in terms of droplet and particulate density, improve as predicted by the theoretical models.

Acknowledgments

The authors are grateful to Dr M. L. De Giorgi for the sharp comments and suggestions, Dr Miguel Oliveira for XPS analyses and to Prof. G. Leggieri for RBS measurements. The authors were also supported by the TMR – access to large scale facilities (Contract No. ERBFHGECT950021) during their visit to the UV Laser Facility (ULF) at Forth.

References

- [1] S. Acquaviva, E. D'Anna, M. L. De Giorgi, G. Leggieri, A. Luches, G. Majni, M. Martino, A. Perrone, J. Zemek, A. Zocco, *Advantages in Science and Technology* **20**, 181 (1998)
- [2] R. Maeda, K. Kikuch, *Surface Engineering* **13**, 71 (1997)
- [3] A. Miotello, R. Kelly, *Appl. Phys. Lett.* **67** (24) 3535 (1995)
- [4] W. Kautek, J. Krüger, M. Lenzner, S. Sartania, C. Spielmann, F. Krausz, *Appl. Phys. Lett.* **69** (21), 3146 (1996)
- [5] X. Liu, D. Du, G. Mouron, *IEEE Journal of Quantum Electronics* **33** 10, 1707 (1997)
- [6] B. N. Chichkov, C. Momma, S. Nolte, F. von Alvensleben, A. Tünnermann, *Appl. Phys. A* **63** 109 (1996)
- [7] K. Sokolowski-Tintem, J. Bialkowski, A. Cavallieri, D. von der Linde, A. Oparim, J. Meyer-ter-Vehn, S. I. Anisimov, *Phys. Rev. Lett.* **81** (1) 224 (1998)
- [8] T. Goetz, M. Stuke, *Appl. Phys. A* **64**, 6 539 (1997)
- [9] I. Zergioti, M. Stuke, *Appl. Phys. A* **67**, 4 391 (1998)
- [10] W. Kautek, J. Kruger, M. Lenzner, S. Sartania, C. Spielmann, F. Krausz, *Appl. Phys. Lett.* **69**, 21 3146 (1996)
- [11] J. Kruger, W. Kautek, *Laser Physics* **9**, 1 30 (1999)
- [12] K. G. Kreider, M. J. Tarlov, G. J. Gillen, G. E. Poirer, L. H. Robins, L. K. Ives, W. D. Bowers, R. B. Marinenko, D. T. Smith, *J. Mat. Res.* **10**, 3079 (1995)
- [13] D. Li, Y. W. Chung, S. Yang, M. S. Wong, F. Adibi, W. D. Sproul, *J. Vac. Sci. Technol. A* **12**, 1470 (1994)
- [14] C. M. Sung, M. Sung, *Mater. Chem. Phys.* **43**, 1 (1989)
- [15] Y. Yonezawa, T. Minamikawa, K. Motsuda, K. Takezawa, A. Morimoto, T. Shimizu, *Appl. Surf. Sci.* **127-129**, 639 (1998)
- [16] K. H. Song, X. Xu, *Appl. Surf. Sci.*, **127-129** 111 (1998)
- [17] A. Semerok, C. Chaleard, V. Detalle, S. Kocon, J. L. Lacour, P. Manchien, P. Meynadier, C. Nouvellon, P. Palianov, M. Perdrix, G. Petite, B. Salle, *Proc. SPIE* **3343**, 1049 (1998)
- [18] M. L. De Giorgi, G. Leggieri, A. Luches, M. Martino, A. Perrone, A. Zocco, G. Barucca, G. Majni, E. Gyorgy, I. N. Mihailescu, M. Popescu, *Appl. Surf. Sci.* **127-129**, 481 (1998)
- [19] N. Nakayama, Y. Tsushiya, S. Tamada, K. Kosuge, S. Nagata, K. Takahiro and S. Yamaguchi, *Jpn. Journal Appl. Phys. Lett.* **32**, L1465 (1993)
- [20] D. Lin-Vien, N. B. Colthup, W. G. Fateley and J. G. Grasselli, *The Handbook of Infrared and Raman Characteristic Frequencies of Organic Molecules*, Academic Press, Inc., (1991)
- [21] A. Zocco, A. Perrone, A. Luches, R. Rella, A. Klini, I. Zergioti, C. Fotakis, *Thin Solid Films* **349**, 100 (1999)
- [22] A. Zocco, A. Perrone, E. D'Anna, G. Leggieri, A. Luches, A. Klini, I. Zergioti, C. Fotakis, *Diam. Rel. Mater.* **8**, 582 (1999)
- [23] C. Chaleard, V. Detalle, S. Kocon, J. L. Lacour, C. Nouvellon, P. Manchien, B. Salle, A. Semerok, *Proc. SPIE* **3404**, 432 (1997).